Speed-dependent line-shape models analysis from molecular dynamics simulations: The collision regime

P. N. M. Hoang, P. Joubert, and D. Robert
Laboratoire de Physique Moléculaire, UMR CNRS 6624, Faculté des Sciences, La Bouloie, Université de Franche-Comté, 25030 Besançon Cedex, France

(Received 8 March 2001; published 14 December 2001)

A spectral line-shape model accounting for the speed dependence of the relaxation parameters has been proposed for the collision regime [D. Robert *et al.*, Phys. Rev. A **47**, R771 (1993)]. In this model, the speed class exchanges are governed by a memory parameter playing a crucial role. It has been exhaustively used to accurately describe the observed inhomogeneous features of H_2 vibration line profiles in various mixtures with respect to concentration and temperature. Molecular dynamics calculations of the characteristic memory parameter are performed in order to test this model from first principles. The resulting data are in remarkable agreement with those deduced from experiments through the model.

DOI: 10.1103/PhysRevA.65.012507 PACS number(s): 33.70.Jg

I. INTRODUCTION

Over the last decade, high-resolution infrared, Raman, and millimeter wave coherent transient studies in gases have revealed the need to include the speed dependence of the collisional relaxation processes in spectral line-shape models [1–4]. This is particularly required for applications in atmospheric physics and optical diagnostics in combustion.

For most molecules at atmospheric or higher pressure, the line mixing due to the overlap of spectral components inside a band must also be accounted for. Recently, May [5] proposed a treatment of Dicke narrowing and other speed-dependent contributions to spectral profiles in terms of the transport relaxation equation. With co-workers, he has also shown [6] that Dicke narrowing [7] of a single line may be treated in exactly the same way as line mixing and has indicated the numerical technique to use. An important step toward having appropriate tools to calculate the spectra with speed-dependent broadening, shifting, and line mixing has been made. Nevertheless, an accurate description of the spectral line shapes basically requires a consistent speed-dependent model for isolated lines. The most recent applications [8–11] use simple speed-dependent extensions of the very well known hard and soft line profiles [12,13] introduced a long time ago to account for the Dicke narrowing [7]. Apart from the fact that these two limit cases are not *a priori* convenient for most molecular systems, more crucially, they are unable to describe well *both* the velocity orientation (for the confinement narrowing) and the speed (velocity modulus) memory effects (for the speed dependence of the collisional relaxation processes). So, besides the necessity of useful empirical models, it appears that further studies of the impact of the velocity memory (*both* orientation *and* modulus) mechanisms on the spectral line-shape models are needed, for various molecular systems and in a wide range of pressures and temperatures.

Toward this goal, we have first studied [14] the speed memory mechanism from the numerical resolution of the kinetic impact equation by using a realistic model for the speed memory function [15]. An extension to the velocity memory has recently been performed [16]. To gain an understanding of these memory mechanisms, free of memory function models, molecular dynamics simulations (MDS) have been carried out. It is well known that, in general, speed and velocity orientation memory processes must be described by specific mechanisms and that, for each of them, the hard and soft limits [12,13] are not *a priori* relevant. Of course, for practical applications, the need for phenomenological analytical models requires the use of pertinent approximations based on such well established and very useful limits [17,18]. But accurate modeling of the spectral line shapes also requires a further understanding of the spectral consequences of the velocity *and* speed memory mechanisms in the Dicke regime. The case of H_2 highly diluted in mixtures with heavy atoms or molecules is particularly illustrative of this last point. Indeed, it is known that the H_2 velocity memory is lost after each collision for such pairs, so that the hard collisional model is relevant. In contrast, it has been shown from comparison between experiments and phenomenological models [3,19] that the same approximation for the velocity modulus is irrelevant, since the speed memory process is close to the soft limit [14]. The use of the hard approximation for the speed would lead, in the collision regime, to an underestimation of about 100% of the observed H_2 linewidth at atmospheric or higher pressure in H_2-X mixtures ($X = N_2$ or Ar) [20,21] since the speed inhomogeneous effect disappears in the hard limit due to the efficiency of the speed changing collisions [17,18].

For the sake of clarity, this paper is devoted to the collision regime, where only the speed memory mechanism is implied through the speed dependence of the relaxation parameters and the collisional speed class exchange mechanism. A phenomenological spectral line-shape model, namely, the RTBT model (cf. Ref. [19]), has been previously proposed for this regime.

The aim of the present paper is to further test this model by direct confrontation between the memory parameter extracted from experimental data for H_2 in various mixtures with respect to concentration and temperature through the RTBT model, with MDS-calculated values. In Sec. II, the

main characteristics of the RTBT model and of the MDS method are presented. Thus (Sec. III), the MDS results for the velocity and speed memory processes of H_2 in various H_2-X mixtures ($X \equiv$ He, Ne, Ar, N_2) with respect to concentration and temperature, as well as the resulting data for x, are given and compared with those obtained from experiments through the RTBT model. Concluding remarks are given in Sec. IV.

II. RTBT MODEL AND MDS FEATURES

A. RTBT line profile

The analytic expression for the RTBT line profile may be defined as [19]

$$I(\omega) = \pi^{-1}\,\mathrm{Re}\left\{\frac{\langle [F(v)]^{-1}\rangle}{1-\langle [x\nu_{\mathrm{Kin}} - x\gamma_{\mathrm{coll}}(v) - ix\delta_{\mathrm{coll}}(v)][F(v)]^{-1}\rangle}\right\}, \tag{1}$$

where

$$F(v) = x\nu_{\mathrm{Kin}} + (1-x)\gamma_{\mathrm{coll}}(v) + i[\tilde{\omega} + (1-x)\delta_{\mathrm{coll}}(v)]. \tag{2}$$

In Eqs. (1) and (2), $\langle \cdots \rangle$ means a Boltzmann average over the v radiator speed, $\tilde{\omega}$ is the detuning angular frequency counted from the ω_0 resonant angular frequency of the radiator ($\tilde{\omega} = \omega - \omega_0$), ν_{Kin} is the total v-independent collisional frequency, $\gamma_{\mathrm{coll}}(v)$ and $\delta_{\mathrm{coll}}(v)$ are the v-dependent line broadening half width at half maximum (HWHM) and line shift, respectively, and the x parameter is the fraction of collisions which induces speed class exchanges. This parameter, defined as the ratio of the velocity and speed time correlations [$x = \tau_{\vec{v}}/\tau_v = \nu_v/\nu_{\vec{v}}$, where $\nu_{\vec{v}}$ ($\equiv \nu_{\mathrm{Kin}}$) and ν_v are, respectively, the velocity and speed changing collision frequency], is called "memory parameter" (cf. Ref. [14]).

The RTBT model is characterized by four temperature-dependent parameters: $\gamma_{\mathrm{coll}}(T)$, $\delta_{\mathrm{coll}}(T)$ [or, equivalently $\gamma_{\mathrm{coll}}(v), \delta_{\mathrm{coll}}(v)$ through pertinent Boltzmann averages; cf. Refs. [1,22,23]], $x(T)$, and $\nu_{\mathrm{Kin}}(T)$. This last parameter is set [3,23] equal to the value calculated from the kinetic theory (KT) [24,25] [i.e., $\nu_{\vec{v}}^{\mathrm{RTBT}}(T) \equiv \nu_{\vec{v}}^{\mathrm{KT}}(T)$]. The collisional shift $\delta_{\mathrm{coll}}(T)$ is directly deduced from the experimental line shapes through the determination of the gravity center of the asymmetric line [23]. The collisional broadening is obtained from the observed broadening γ_{obs}, through the study of its dependence on the concentration of C [$\gamma_{\mathrm{obs}}(C) = \gamma_{\mathrm{coll}}(C) + \gamma_{\mathrm{inh}}(C)$, where γ_{inh} denotes the inhomogeneous broadening resulting from the speed dependence of the relaxation parameters]. The inhomogeneous broadening γ_{inh} exhibits a nonlinear dependence on concentration, in contrast with $\gamma_{\mathrm{coll}}(C)$, which is linear, as is well known. The x memory parameter is determined from the fit of $\gamma_{\mathrm{obs}}(C)$. Notice that for all the H_2-X mixtures considered here, $\gamma_{\mathrm{coll}}(T)$ is linear with respect to the temperature [$\gamma_{\mathrm{coll}}(T) = \tilde{\gamma}T + \gamma_0$]. So that, in practice, three parameters are fitted from $\gamma_{\mathrm{obs}}(C)$ (i.e., x, $\tilde{\gamma}$, and γ_0) at each temperature. Furthermore, since $\delta_{\mathrm{coll}}(T) = \tilde{\delta}\sqrt{T} + \delta_0$ for these mixtures, five parameters are experimentally determined at each temperature, two from direct measurements of the line profile through its gravity center ($\tilde{\delta}$ and δ_0), three from a fit of $\gamma_{\mathrm{obs}}(C)$ (x, $\tilde{\gamma}$, and γ_0). The accuracy of these last three parameters, and thus that of $x(T)$ and $\gamma_{\mathrm{coll}}(T)$, is consequently well correlated. Through the exhaustive previous studies of binary H_2-X mixtures [3,20,21,23,26–28], the four parameters ($\tilde{\delta}, \delta_0, \tilde{\gamma}, \gamma_0$), plus $x(T)$, have been determined for several H_2-X molecular pairs, in particular for X = He, Ne, Ar, and N_2.

TABLE I. Atom-atom Lennard-Jones parameters [25,32] for the well depth ε and molecular diameter σ. The quadrupole is 0.484 a.u. for H_2 molecule and −0.966 a.u. for N_2 [33].

	H-H	H-He	H-Ne	H-N	H-Ar	N-N
ε (K)	11.25	10.61	19.85	33.64	36.75	36.35
σ (Å)	2.69	2.64	2.72	3.19	3.04	3.35

In Eqs. (1) and (2), $x\nu_{\mathrm{Kin}}$, $x\gamma_{\mathrm{coll}}$, $x\delta_{\mathrm{coll}}$, $(1-x)\gamma_{\mathrm{coll}}$, and $(1-x)\delta_{\mathrm{coll}}$ are linearly dependent on perturber concentration. This allows one to straightforwardly describe the RTBT model for the case of two (or three, cf. Ref. [26]) collisional partners (within the impact approximation). If $c_{\mathrm{H_2}}$ and c_X mean the concentration of the two species in binary mixtures, the expression for any of them is (for $x\nu_{\mathrm{Kin}}$, for instance)

$$x\nu_{\mathrm{Kin}} = [c_{\mathrm{H_2}} x_{\mathrm{H_2}} \tilde{\nu}_{\mathrm{Kin}}^{\mathrm{H_2}} + c_X x_X \tilde{\nu}_{\mathrm{Kin}}^{X}]\rho, \tag{3}$$

where ρ is the total density (in amagat) and $\tilde{\nu}_{\mathrm{Kin}}^{X}$ is the total collisional frequency per density unit for H_2-X (in $\mathrm{cm}^{-1}\,\mathrm{amagat}^{-1}$).

Let us mention that in the beginning of this exhaustive experimental study of H_2-X by Berger and co-workers [3,23], with the temperature being restricted to less than 1000 K, the need for speed dependence for γ_{coll} within the RTBT model [19] [cf. Eqs. (1) and (2)] was not required in order to get an accurate description of the observed line shapes. Further studies at 1200 K [28] have revealed the need to also introduce, besides the $\delta_{\mathrm{coll}}(v)$ law, the $\gamma_{\mathrm{coll}}(v)$ one. As a consequence, the $x_{\mathrm{expt}}^{\mathrm{RTBT}}(T)$ values have been significantly modified with respect to those of Refs. [3,23], due to the above-mentioned correlation between these values and those of $\gamma_{\mathrm{coll}}(T)$ (through $\tilde{\gamma}$ and γ_0; cf. supra). In the further analysis performed by Chaussard *et al.* [20,21], the experimental profiles have been first reanalyzed at high density by using $\delta_{\mathrm{coll}}(v)$ and $\gamma_{\mathrm{coll}}(v)$ laws (cf. step 1′ in Table 1 of Refs. [20,29]. The $x_{\mathrm{expt}}^{\mathrm{RTBT}}(T)$ values used for a comparison with MDS data in the following section are thus these revisited values.

B. Details of the simulation

The molecular dynamics calculations of the autocorrelation velocity function $\varphi_{\vec{v}}(t)$ and of the centered speed autocorrelation function $\varphi_{v-\langle v\rangle}(t)$ (where $\langle v\rangle$ is the mean speed) were carried out by standard methods in a cubic simulation

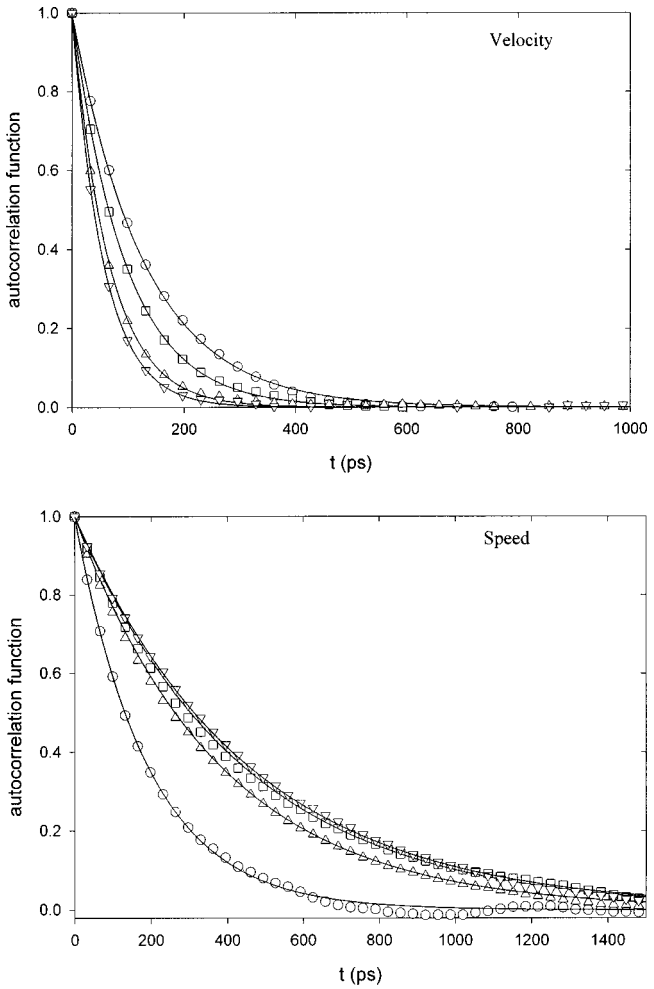

FIG. 1. H_2 velocity normalized autocorrelation function $\varphi_{\vec{v}}(t)=\langle\vec{v}(0)\vec{v}(t)\rangle/\langle\vec{v}^2(0)\rangle$ (a) and centered speed normalized autocorrelation function $\varphi_{v-\langle v\rangle}(t)=\langle[v(0)-\langle v\rangle][v(t)-\langle v\rangle]\rangle/\langle[v(0)-\langle v\rangle]^2\rangle$ (b) obtained from MDS at 300 K and 5 amagat (but given here for clarity at 1 amagat) vs time (in picoseconds). ○, H_2-He; □, H_2-Ne; △, H_2-N_2; and ▽, H_2-Ar. Solid line: exponential fit.

box. Periodic boundary conditions were used in the *x,y,z* plane. The side of this box was 287.64 Å. A total number of $N=2916$ particles (H_2 molecules$+X$ perturbers) was considered in all simulations. This quite large number of particles together with the size of the simulation box ensures good statistics at a density of 5 amagat, even when a weak concentration of H_2 is implied.

At the start of each simulation run, N perturbers are placed at c.f.c. lattice sites in the box. Then, depending on the desired concentration of $C_{H_2}=N_{H_2}/N$ in hydrogen, N_{H_2} hydrogen molecules with random orientations are scattered in the box, replacing N_{H_2} perturbers. The hydrogen and nitrogen molecules are treated as classical rigid rotors, and five external coordinates are used to describe the translation of the center of mass and its orientation with respect to an absolute frame tied to the bottom of the simulation box. The translational equations of motion are solved using the Verlet algorithm, and a predictor-corrector method based on the quaternion representation of the molecular orientations is used for the orientational equations [30] with a time step of 5 fs. Every run involved an equilibration period of 40 000 steps, followed by a production run of 300 000 steps corresponding to a duration of 1.5 ns of simulation.

The initial linear and angular velocities (in the case of H_2 and N_2) for all moving molecules are taken from a Boltzmann distribution corresponding to the desired simulation temperature. This temperature is held constant during the production runs by scaling the velocities every 15 steps. Tests showed that the results obtained with this rescaling procedure were not significantly different from runs done within the microcanonical ensemble [31]. The cutoff in the calculations of the H_2-H_2,H_2-perturber and perturber–perturber interactions is handled through three different neighbor lists [32], with the same radial cutoff.

The dispersion-repulsion interactions are described by an atom-atom Lennard-Jones potential in all cases. The electrostatic quadrupole-quadrupole interaction, acting on the center of mass, is additionally used in the case of H_2-H_2 and H_2-N_2. Table I gives the parameters for these interactions. It has been checked that the rotational motion, treated classically and not quantally as rigorously required for H_2, does not significantly change $\tau_{\vec{v}}$ and τ_v (within a few percent).

TABLE II. Comparison between velocity-changing frequency $\nu_{\vec{v}}^{\mathrm{MDS}}$ ($\nu_{\vec{v}}=\tau_{\vec{v}}^{-1}/2\pi c$, where c is the speed of light) deduced from the present molecular dynamical study (MDS) from an exponential fit (cf. Fig. 1) and $\nu_{\vec{v}}^{\mathrm{KT}}$ calculated from the kinetic theory [24,25] by using data of Table III at 300 K. The speed-changing collision frequency ν_v^{MDS} ($\nu_v=\tau_v^{-1}/2\pi c$) obtained from MDS is also reported. The fraction $x=\nu_v/\nu_{\vec{v}}$ of speed changing collision among the velocity ones x^{MDS} for MDS and experiments, through the RTBT model, $x_{\mathrm{expt}}^{\mathrm{RTBT}}$, are given. Frequencies are expressed in 10^{-3} cm^{-1} amagat^{-1}. The memory parameter x is dimensionless.

	H_2-H_2	H_2-He	H_2-Ne	H_2-N_2	H_2-Ar
$\nu_{\vec{v}}^{\mathrm{MDS}}$	48.3	41.0	56.5	82.1	97.2
$\nu_{\vec{v}}^{\mathrm{KT}}$	50.7	45.7	62.0	94.8	93.1
ν_v^{MDS}	49.2	27.0	10.2	12.2	9.8
x^{MDS}	1.0	0.66	0.18	0.15	0.10
$x_{\mathrm{expt}}^{\mathrm{RTBT}}$ [3,20,21,26]	1.0	0.68	0.14	0.14	0.10

III. MDS RESULTS AND COMPARISON WITH EXPERIMENT

A. General features of MDS results

Figure 1 gives the time dependence of the normalized velocity and centered speed autocorrelation function (ACF) $\varphi_{\vec{v}}(t)$ and $\varphi_{v-\langle v\rangle}(t)$ at concentration $C_{H_2}=0.05$ for H_2 in H_2-X mixtures ($X\equiv$He, Ne, N_2,Ar) at 300 K. Apart from the expected ACF exponential decrease from gas kinetic theory [24,25] and also from the expected decrease of the velocity correlation time $\tau_{\vec{v}}$ from He to Ar, the main feature is the strong increase of τ_v from He to N_2, Ne and Ar. The MDS velocity $\nu_{\vec{v}}^{\mathrm{MDS}}$ and speed ν_v^{MDS} frequency in the high dilution

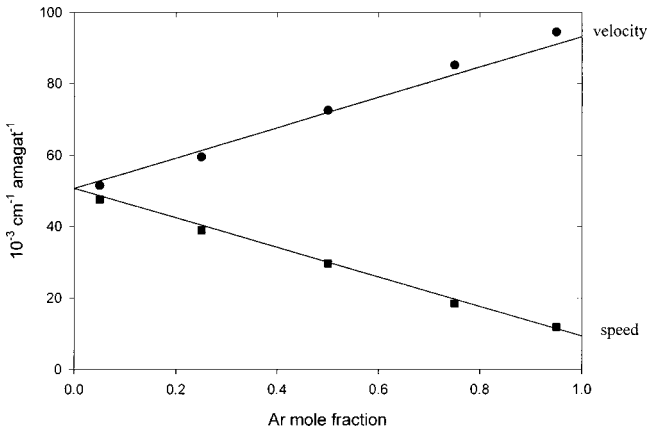

FIG. 2. H_2-Ar velocity changing collisions frequency $\nu_{\vec{v}}$ and speed changing collisions frequency $\nu_{\vec{v}}$ vs Ar mole fraction at 300 K and 5 amagat. Comparison between the present MDS results (●: $\nu_{\vec{v}}$ and ■: $\nu_{\vec{v}}$) and the RTBT model (—).

limit have been gathered in Table II, as well as the resulting $x=\nu_{\vec{v}}/\nu_{\vec{v}}$ memory parameter. These x^{MDS} values are fully consistent with those deduced from stimulated Raman scattering (SRS) experiments [3,20,21,26–28] at high density (i.e., in the collision regime), through the RTBT model.

Table II also shows that for pure H_2, $x_{H_2}^{\mathrm{MDS}}\cong 1$. Notice that for all the previous H_2-X mixture studies, this $x_{H_2}^{\mathrm{RTBT}}=1$ value has been used in Eq. (3). This was suggested by the absence of an asymmetry for the observed isotopic Raman $Q(J)$ lines [23] in pure H_2. For this purpose, let us mention that the presence of speed-inhomogeneous effects in H_2-X spectral line shapes manifests itself as an asymmetric profile and as a nonlinearity of the observed line broadening with respect to concentration [1,3]. A second interesting check is the H_2-He case. Indeed, for this mixture and contrary to the others, neither significant line asymmetry nor nonlinear broadening with respect to C_{H_2} was observed [23,27], so that a range of values for x lying between 0.5 and 1 was convenient. A recent study of H_2-He-Ar and H_2-He-N_2 ternary mixtures [26] has allowed one to determine accurately this x_{He} value, which is equal to 0.68 at 300 K. This value is to be compared with the MDS value ($x_{\mathrm{He}}^{\mathrm{MDS}}=0.66$, cf. Table II).

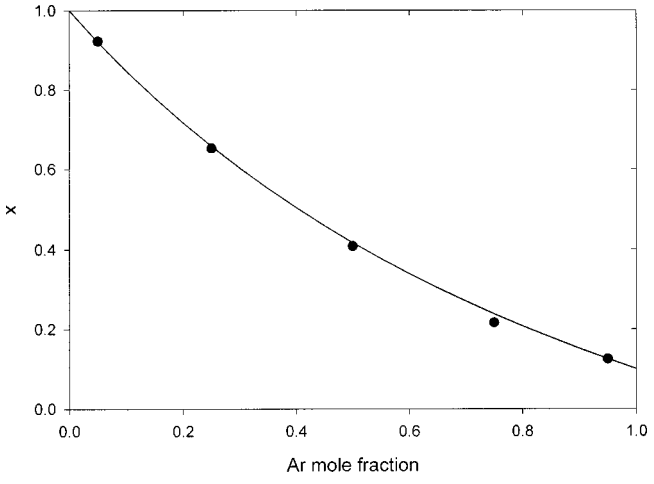

FIG. 3. H_2-Ar fraction of speed changing collisions among the velocity ones ($x=\nu_v/\nu_{\vec{v}}$) vs Ar mole fraction at 300 K. Comparison between results obtained from the present MDS results (●) and the RTBT model (—).

TABLE III. Isotropic Lennard-Jones potential parameters for different colliding partners deduced from a fit to the atom-atom potential model (cf. Table I).

	H_2-H_2	H_2-He	H_2-Ne	H_2-N_2	H_2-Ar
ε (K)	33.5	18.1	34.0	57.5	64.8
σ (Å)	2.93	2.77	2.84	3.32	3.16

B. Concentration and temperature dependence of the memory parameter

In order to test further the RTBT model from *ab initio* data, a MDS study of $\nu_{\vec{v}}$ and ν_v collision frequency with respect to concentration has been performed for the H_2-Ar mixture. The resulting MDS data (Fig. 2) exhibits the expected linearity of $\nu_{\vec{v}}$ and ν_v vs $C_{\mathrm{Ar}}=1-C_{H_2}$. Their comparison with the values calculated from the kinetic theory [24,25], using the binary collisional linear law with respect to concentration $[\nu_{\vec{v}}^{\mathrm{KT}}(C_{\mathrm{Ar}})=(1-C_{\mathrm{Ar}})(\nu_{\vec{v}}^{\mathrm{KT}})_{H_2}+C_{\mathrm{Ar}}(\nu_{\vec{v}}^{\mathrm{KT}})_{\mathrm{Ar}}]$, shows a high consistency with the RTBT values. Similarly, we have reported in Fig. 2 the experimental values for $\nu_v(C_{\mathrm{Ar}})$ [calculated from $\nu_v(C_{\mathrm{Ar}})=(1-C_{\mathrm{Ar}})x_{H_2}(\nu_{\vec{v}})_{H_2}+C_{\mathrm{Ar}}x_{\mathrm{Ar}}(\nu_{\vec{v}})_{\mathrm{Ar}}$] by using for x_{Ar} the experimental data deduced from the RTBT model (cf. Refs. [20,29] and comments in Sec. II A). The agreement between MDS and RTBT data exhibits the same consistency as for $\nu_{\vec{v}}$.

An additional proof is obtained through the analysis of the concentration dependence of the memory parameter for the H_2-Ar mixtures, i.e., $x(C_{\mathrm{Ar}})=\nu_v(C_{\mathrm{Ar}})/\nu_{\vec{v}}(C_{\mathrm{Ar}})$. Figure 3 shows that this dependence is nonlinear and that the consistency with the RTBT data remains remarkable.

In order to complete this comparison between experimental data for the x memory parameter obtained from the RTBT model and the present MDS results, we have performed molecular dynamics simulation for H_2-Ar with respect to temperature at $C_{H_2}=0.05$. The agreement between MDS $\nu_{\vec{v}}$ values and those calculated from the kinetic theory (cf. Table III) is excellent (Table IV), allowing one to be confident of

TABLE IV. Comparison between results obtained in a mixture of 5% H_2 in 95% Ar from the present MDS study and the experimental data obtained from the RTBT model for the velocity changing collision frequency $\nu_{\vec{v}}$ and the speed changing one ν_v vs temperature. The frequencies are expressed in 10^{-3} cm^{-1} amagat^{-1}.

T (K)	$\nu_{\vec{v}}^{\mathrm{MDS}}$	$\nu_{\vec{v}}^{\mathrm{RTBT}}\equiv\nu_{\vec{v}}^{\mathrm{KT}}$	ν_v^{MDS}	ν_v^{RTBT}
300	94.5	91.0	11.8	12.3
600	93.2	111.5	11.0	10.9
900	102.6	125.6	11.5	10.7
1200	124.8	136.6	11.6	10.6

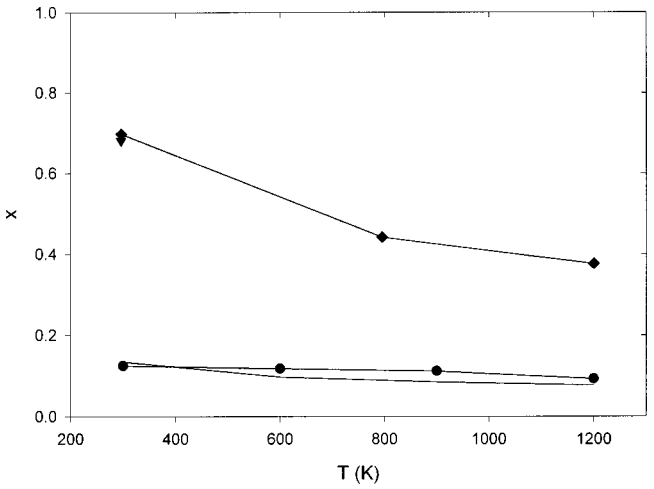

FIG. 4. H_2-Ar fraction of speed-changing collisions among the velocity ones ($x=\nu_v/\nu_{\bar{v}}$) vs temperature for a mixture of 5% H_2 in 95% Ar. Comparison between results obtained from the present MDS study (●) and the RTBT model (—). For comparison, the results obtained for H_2-He mixture are also reported (▼: MDS and ◆: RTBT). N.B.: The MDS data for H_2-He at high temperature have not been reported because of the lightness of He which requires exhaustive CPU time.

theMDS data at high temperature for ν_v $(T, C_{H_2}=0.05)$. The resulting data for the $x(T)$ memory parameter with respect to temperature are reported in Fig. 4 and compared with the RTBT data.

IV. CONCLUSION AND DISCUSSION

The present MDS results show that the RTBT model [19], not only accurately describes the experimental SRS profiles in the collision regime, as previously established [3,23,26–28], but that the characteristic speed memory parameter $x(T)$ has a well defined physical meaning. This parameter, which governs the collisional speed class exchanges in this model, is the ratio of the velocity and the speed correlation times. Indeed, high consistency is obtained between these MDS results and the RTBT data. This consistency concerns the dependence of the memory parameter on the nature of the perturber, as well as its dependence on the concentration and temperature for all the considered H_2-X mixtures ($X \equiv$ He, Ne, Ar, N_2). Furthermore, since the accuracy of the experimentally determined $\gamma_{\mathrm{coll}}(T)$ law is highly correlated to that of the $x(T)$ parameter (cf. Sec. II A), the present MDS study is also a check for the accuracy of this $\gamma_{\mathrm{coll}}(T)$ law deduced from SRS profiles through the RTBT model $[\gamma_{\mathrm{coll}}(T)=\tilde{\gamma}T+\gamma_0]$.

Such a consistency between theory and experiment requires an examination of the basic assumption underlying the RTBT model [19]. This model accounts for the statistical dependence of the radiator velocity and phase changes, since they can arise in the same collision. But the values of these changes are considered to be in no way intercorrelated [13]. The role of such a correlation between collision-induced changes in the internal quantum states and the radiator velocity has been carefully analyzed by Berman [35–37] and by Nienhuis [38]. It may become important when the intermolecular potential energy V_i and V_f strongly differs in the two quantum states $|i\rangle$ and $|f\rangle$ involved in the optical transition. This means that a large difference in these two potentials may lead to significantly different classical trajectories. This quantum effect implies that collisions must be rigorously considered as state selecting, resulting in a decrease of Dicke narrowing and an increase of collisional broadening. Such state-selecting collisions have not been accounted for either in the RTBT model or in the (purely classical) MDS calculations. The obtained agreement with experimental profiles for the $Q(J)$ lines' profiles of the H_2-X mixtures considered ($X \equiv$ He, Ne, Ar, and N_2) in the collision regime seems to indicate that the V_i and V_f potentials are sufficiently close that the resulting collision-induced phase perturbation η_{fi} is much weaker than unity.

Since the rovibrational relaxation process is highly dominated by the vibrational dephasing for the above H_2-X systems [39], the inelastic rotational contributions will be disregarded in the following discussion. The vibrational phase shift $\eta_{fi}(b,v_r)$ has been previously calculated for these H_2-X systems versus the impact parameters b and the relative velocity v_r (cf. Fig. 3 of Ref. [40]). The results clearly justify the use of the approximation of weak phase perturbation ($\eta_{fi} \ll 1$) for temperatures above room temperature and, concomitantly, the neglect of the correlation between internal rovibrational quantum changes and the radiator velocity. Particular attention must be paid to the extension of such an approximation to other systems by checking its validity.

Finally, let us mention that the present comparison has been restricted to the collision regime. For many applications, the Dicke regime is also of interest. An extension of the RTBT model [19], accounting thus not only for the speed dependence of the relaxational parameter and of the speed class exchanges, but also for the collisional confinement narrowing, has been recently proposed [17]. This model has allowed one to accurately describe H_2 vibrational line profiles in various mixtures for a wide range of pressure and temperature [20,21], in spite of the fact that it does not discriminate between velocity-orientation and velocity-modulus memory processes, as rigorously required [41]. A future paper will be devoted to an analysis of this more general spectral line-shape model [17] from MDS data and to the development of a refined approach where the velocity-modulus and the velocity-orientation memory mechanisms are specifically accounted for.

[1] R. L. Farrow, L. A. Rahn, G. O. Sitz, and G. J. Rosasco, Phys. Rev. Lett. **63**, 746 (1989).

[2] P. Duggan, P. M. Sinclair, M. P. Le Flohic, J. W. Forsman, R. Berman, A. D. May, and J. R. Drummond, Phys. Rev. A **48**, 2077 (1993).

[3] J. Ph. Berger, R. Saint-Loup, H. Berger, J. Bonamy, and D. Robert, Phys. Rev. A **49**, 3396 (1994).

[4] F. Rohart, H. Mäder, and H. W. Nicolaisen, J. Chem. Phys.

101, 6475 (1994).
[5] A. D. May, Phys. Rev. A **59**, 3495 (1999).
[6] S. Dolbeau, R. Berman, J. R. Drummond, and A. D. May, Phys. Rev. A **59**, 3506 (1999).
[7] R. H. Dicke, Phys. Rev. **89**, 472 (1983).
[8] A. Henry, D. Hurtmans, M. Margotin-Maclou, and A. Valentin, J. Quant. Spectrosc. Radiat. Transf. **56**, 647 (1996).
[9] B. Lance, G. Blanquet, J. Walrand, and P. Bouanich, J. Mol. Spectrosc. **185**, 262 (1997).
[10] R. Berman, P. M. Sinclair, A. D. May, and J. R. Drummond, J. Mol. Spectrosc. **197**, 283 (1999).
[11] D. Priem, F. Rohart, J. M. Colmont, G. Wlodarczak, and J. P. Bouanich, J. Mol. Struct. **517**, 435 (2000).
[12] L. Galatry, Phys. Rev. **122**, 1218 (1961).
[13] S. G. Rautian and I. I. Sobelman, Usp. Fiz. Nauk **90**, 209 (1966); Sov. Phys. Usp. **9**, 701 (1967).
[14] D. Robert and L. Bonamy, Eur. Phys. J. D **2**, 245 (1998).
[15] J. Keilson and J. E. Storer, Q. Appl. Math. **10**, 243 (1952).
[16] L. Bonamy, P. Joubert, and D. Robert (unpublished).
[17] B. Lance and D. Robert, J. Chem. Phys. **109**, 8283 (1998); **111**, 789 (1999).
[18] R. Ciurylo and S. Szudy, J. Quant. Spectrosc. Radiat. Transf. **57**, 411 (1997); R. Ciurylo, Phys. Rev. A **58**, 1029 (1998); R. Ciurylo, A. S. Pine, and S. Szudy, J. Quant. Spectrosc. Radiat. Transf. **67**, 375 (2000).
[19] D. Robert, J. M. Thuet, J. Bonamy, and S. Temkin, Phys. Rev. A **47**, R771 (1993).
[20] F. Chaussard, X. Michaut, H. Berger, P. Joubert, B. Lance, J. Bonamy, and D. Robert, J. Chem. Phys. **112**, 158 (2000).
[21] F. Chaussard, R. Saint-Loup, H. Berger, P. Joubert, X. Bruet, J. Bonamy, and D. Robert, J. Chem. Phys. **113**, 4951 (2000).
[22] H. M. Pickett, J. Chem. Phys. **73**, 6090 (1980).
[23] J. Ph. Berger, Ph.D. thesis, Université de Bourgogne, France, 1994.
[24] S. Chandrasekhar, Rev. Mod. Phys. **15**, 1 (1943).
[25] J. O. Hirschfelder, C. F. Curtiss, and R. B. Bird, in *Molecular Theory of Gases and Liquids* (Wiley, New York, 1964).
[26] P. Joubert, X. Bruet, J. Bonamy, D. Robert, F. Chaussard, R. Saint-Loup, and H. Berger, J. Chem. Phys. **113**, 10056 (2000).
[27] J. Forsman, J. Bonamy, D. Robert, J. Ph. Berger, R. Saint-Loup, and H. Berger, Phys. Rev. A **52**, 2652 (1995).
[28] P. M. Sinclair, J. Ph. Berger, X. Michaut, R. Saint-Loup, H. Berger, J. Bonamy, and D. Robert, Phys. Rev. A **54**, 402 (1996).
[29] F. Chaussard, Ph.D. thesis, Université de Bourgogne, France, 2001.
[30] M. P. Tildesley and D. J. Tildesley, *Computer Simulation of Liquids* (Clarendon, Oxford, 1987).
[31] P. N. M. Hoang, S. Picaud, C. Girardet, and A. W. Meredith, J. Chem. Phys. **105**, 8453 (1996).
[32] S. Picaud and P. N. M. Hoang, J. Chem. Phys. **113**, 9898 (2000).
[33] M. Oobatake and T. Ooi, Prog. Theor. Phys. **48**, 2132 (1972).
[34] J. P. Bouanich, J. Quant. Spectrosc. Radiat. Transf. **47**, 243 (1992).
[35] P. R. Berman, Phys. Rev. A **6**, 2157 (1972).
[36] P. R. Berman, Appl. Phys. **6**, 283 (1975).
[37] P. R. Berman, in *New Trends in Atomic Physics*, edited by Grynberd and Stora, Les Houches (North-Holland, Amsterdam, 1984), Vol. 38, pp. 451–514.
[38] G. Nienhuis, J. Quant. Spectrosc. Radiat. Transf. **20**, 275 (1978).
[39] D. Robert, J. Bonamy, F. Marsault-Herail, G. Levi, and J. P. Marsault, Chem. Phys. Lett. **74**, 467 (1980).
[40] D. Robert, J. Bonamy, J. P. Sala, G. Levi, and F. Marsault-Herail, Chem. Phys. **99**, 303 (1985).
[41] D. Robert, P. Joubert, and B. Lance, J. Mol. Struct. **517-518**, 393 (2000).